4

Dimensionality reduction and phase plane analysis

The firing of action potentials has been successfully described by the Hodgkin–Huxley model, originally for the spikes in the giant axon of the squid but also, with appropriate modifications of the model, for other neuron types. The Hodgkin–Huxley model is defined by four nonlinear differential equations. The behavior of high-dimensional systems of nonlinear differential equations is difficult to visualize – and even more difficult to analyze. For an understanding of the firing behavior of the Hodgkin–Huxley model, we therefore need to turn to numerical simulations of the model. In Section 4.1 we show, as an example, some simulation results in search of the firing threshold of the Hodgkin–Huxley model. However, it remains to show whether we can get some deeper insights into the observed behavior of the model.

Four equations are in fact just two more than two: in Section 4.2 we exploit the temporal properties of the gating variables of the Hodgkin–Huxley model so as to approximate the four-dimensional differential equation by a two-dimensional one. Two-dimensional differential equations can be studied in a transparent manner by means of a technique known as "phase plane analysis." Section 4.3 is devoted to the phase plane analysis of generic neuron models consisting of two coupled differential equations, one for the membrane potential and the other for an auxiliary variable.

The mathematical tools of dimension reduction and phase plane analysis that are presented in Sections 4.2 and 4.3 will be repeatedly used throughout this book, in particular in Chapters 5, 6, 16 and 18. As a first application of phase plane analysis, we study in Section 4.4 the classification of neurons into type I and type II according to their frequency–current relation. As a second application of phase plane analysis, we return in Section 4.5 to some issues around the notion of a "firing threshold," which will be sketched now.

4.1 Threshold effects

Many introductory textbooks of neuroscience state that neurons fire an action potential if the membrane potential reaches a threshold. Since the onset of an action potential is characterized by a rapid rise of the voltage trace, the onset points can be detected in exper-

https://doi.org/10.1017/CBO9781107447615.005 Published online by Cambridge University Press

iment recordings (Fig. 4.1a). Intuitively, the onset of an action potential occurs when the membrane potential crosses the firing threshold.

The firing threshold is not only a useful concept for experimental neuroscience, it is also at the heart of most integrate-and-fire models and therefore central to Parts II and III of this book. But does a firing threshold really exist?

Experimenters inject currents into a single neuron to probe its firing characteristics. There is a large choice of potential current wave forms, but only few of these are routinely used in many labs. In this section we use current pulses and steps in order to explore the threshold behavior of the Hodgkin–Huxley model.

4.1.1 Pulse input

A Hodgkin–Huxley model is stimulated by a short current pulse of 1 ms duration. If the stimulus is strong enough, it elicits a spike. In Fig. 4.1a,b the amplitude of the stimulating current is only slightly increased between the first and second current pulse. The membrane potential returns directly to the resting potential after the stimulus, while the neuron fires a spike in response to the second pulse. This seems to suggest that the voltage threshold for spike firing is just above the maximum voltage that is reached after the first current injection (upper horizontal dashed line in Fig. 4.1b.

Unfortunately, however, such an interpretation is incorrect. If we use a longer current pulse of 100 ms duration and apply the same argument as before, we would find a different voltage threshold, indicated by the lower horizontal dashed line in Fig. 4.1b.

Despite the fact that neuronal action potential firing is often treated as a threshold-like behavior, such a threshold is not well defined mathematically (Rinzel and Ermentrout, 1998; Koch *et al.*, 1995). For practical purposes, however, the transition can be treated as a threshold effect. However, the threshold we find depends on the stimulation protocol.

For a mathematical discussion of the threshold phenomenon, it is helpful to reduce the system of four differential equations to two equations; this is the topic of Section 4.2. We will return to pulse currents in Section 4.5.

Example: Short current pulse as voltage step

The above argument excludes a voltage threshold, but could there be a current threshold? Instead of injecting a current of 1 ms duration we can use a shorter pulse that lasts only half as long. Numerically, we find that the minimal current necessary to trigger an action potential of the Hodgkin–Huxley model is now twice as large as before. We conclude that, for short current pulses, it is not the amplitude of the current that sets the effective firing threshold, but rather the integral of the current pulse or the charge. Indeed, the more charge we put on the membrane the higher the voltage, simply because of the capacitance C of the membrane. For very short current pulses

https://doi.org/10.1017/CBO9781107447615.005 Published online by Cambridge University Press

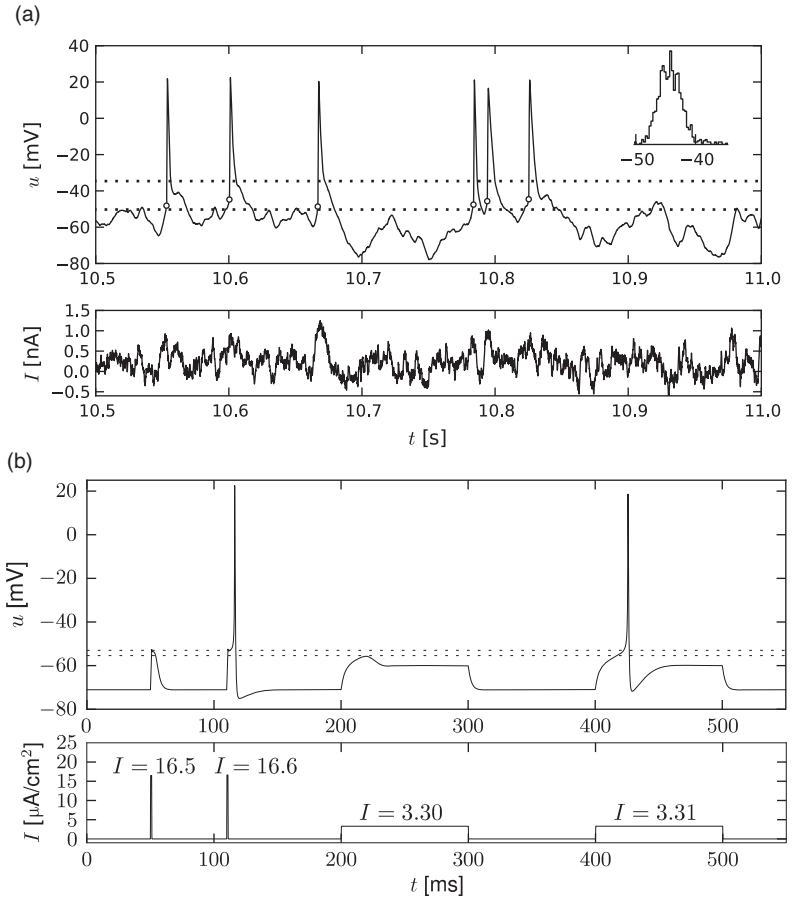

Fig. 4.1 Firing threshold. (a) Experimental recording of membrane voltage (top) during stimulation with a time-dependent current (bottom). The onset of spikes, defined as the moment when the voltage starts its upswing, is marked by open circles. The lowest and highest onset voltage during a recording of 20 s are marked by dotted horizontal lines. Inset: Histogram of onset voltages; adapted from Mensi *et al*. (2013). (b) Stimulation of the Hodgkin–Huxley model with pulse and step current. Voltage (top) in response to pulses and steps (bottom). The apparent voltage threshold is higher (dotted lines in top panel) for a pulse than for a step current. The critical currents are 16.6 μA/cm^2 for the 1 ms pulse and 3.31 μA/cm^2 for the step. Parameters of the Hodgkin–Huxley model as in Table 2.1.

$$I(t) = q\,\delta(t) = \lim_{\Delta\to 0} \frac{q}{\Delta} \quad \text{for } 0 < t < \Delta \quad \text{and 0 otherwise.} \tag{4.1}$$

The voltage of the Hodgkin–Huxley model increases at the moment of current injection by an amount $\Delta u = q/C$ where q is the charge of the current pulse (see Section 1.3.2). If the model was at rest for $t < 0$, the new voltage $u = u_{\rm rest} + \Delta u$ can be used as the initial condition for the numerical integration of the Hodgkin–Huxley model for times

https://doi.org/10.1017/CBO9781107447615.005 Published online by Cambridge University Press

$t > 0$. Thus, a short current pulse amounts to a step-like increase of the voltage by a fixed amount.

4.1.2 Step current input

In Chapter 2 we have seen that a constant input current $I_0 > I_\theta$ can generate regular firing. In this paragraph we study the response of the Hodgkin–Huxley model to a step current of the form

$$I(t) = I_1 + \Delta I\, \Theta(t)\,. \tag{4.2}$$

Here $\Theta(t)$ denotes the Heaviside step function, i.e., $\Theta(t) = 0$ for $t \leq 0$ and $\Theta(t) = 1$ for $t > 0$. At $t = 0$ the input jumps from a fixed value I_1 to a new value $I_2 = I_1 + \Delta I$; see Fig. 4.2a. We may wonder whether spiking for $t > 0$ depends only on the final value I_2 or also on the step size ΔI.

The answer to this question is given by Fig. 4.2d. A large step ΔI facilitates the spike initiation. For example, a target value $I_2 = 2\,\mu\text{A/cm}^2$ elicits a spike, provided that the step size is large enough, but does not cause a spike if the step is small. The letter S in Fig. 4.2d denotes the regime where only a single spike is initiated. Repetitive firing (regime R) is possible for $I_2 > 2.6\,\mu\text{A/cm}^2$, but must be triggered by sufficiently large current steps.

We may conclude from Fig. 4.2d that, when probing with step currents, there is neither a unique current threshold for spike initiation nor for repetitive firing. The trigger mechanism for action potentials depends not only on I_2 but also on the size of the current step ΔI.

Biologically, the dependence upon the step size arises from the different time constants of activation and inactivation of the ion channels. Mathematically, the stimulation with step currents can be analyzed transparently in two dimensions (Sections 4.3 and 4.4).

4.2 Reduction to two dimensions

A system of four differential equations, such as the Hodgkin–Huxley model, is difficult to analyze, so that normally we are limited to numerical simulations. A mathematical analysis is, however, possible for a system of two differential equations.

In this section we perform a systematic reduction of the four-dimensional Hodgkin–Huxley model to two dimensions. To do so, we have to eliminate two of the four variables. The essential ideas of the reduction can also be applied to detailed neuron models that may contain many different ion channels. In these cases, more than two variables would have to be eliminated, but the procedure would be completely analogous (Kepler *et al*., 1992).

4.2.1 General approach

We focus on the Hodgkin–Huxley model discussed in Chapter 2 and start with two qualitative observations. First, we see from Fig. 2.3b that the time scale of the dynamics of the

https://doi.org/10.1017/CBO9781107447615.005 Published online by Cambridge University Press

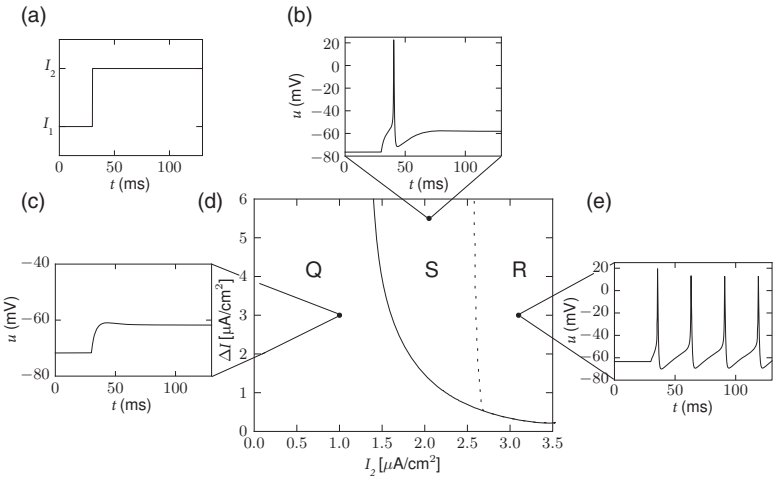

Fig. 4.2 Phase diagram for stimulation with a step current. (a) The input current $I(t)$ changes at $t = 0$ from I_1 to I_2. (b), (c), (e). Sample responses of the Hodgkin–Huxley model to step current input. (d) The outcome of the simulation experiment as a function of the final current I_2 and the step size $\Delta I = I_2 - I_1$. Three regimes denoted by S, R, and Q may be distinguished. In Q no action potential is initiated (quiet regime). In S, a single spike is initiated by the current step (single spike regime). In R, periodic spike trains are triggered by the current step (repetitive firing). Examples of voltage traces in the different regimes are presented in the smaller graphs (b, c, e) with stimulation parameters indicated by the filled circles in (d). Note that for the same final current I_2 (e.g., (d) 2.0 μA/cm^2), the neuron model emits a spike if the current step ΔI is large enough (regime S), or no spike if the step is too small. For a final current $I_2 = 3$ μA/cm^2, the model exhibits bistability between repetitive firing and quiescence.

gating variable m is much faster than that of the variables n and h.Moreover, the time scale of m is fast compared with the membrane time constant $\tau = C/g_L$ of a passive membrane, which characterizes the evolution of the voltage u when all channels are closed. The relatively rapid time scale of m suggests that we may treat m as an instantaneous variable. The variable m in the ion current equation (2.5) of the Hodgkin–Huxley model can therefore be replaced by its steady-state value, $m(t) \to m_0[u(t)]$. This is what we call a *quasi steady-state approximation* which is possible because of the "separation of time scales" between fast and slow variables.

Second, we see from Fig. 2.3b that the time constants $\tau_n(u)$ and $\tau_h(u)$ have similar dynamics over the voltage u. Moreover, the graphs of $n_0(u)$ and $1 - h_0(u)$ in Fig. 2.3a are also similar. This suggests that we may approximate the two variables n and $(1-h)$ by a single effective variable w. To keep the formalism slightly more general we use a linear approximation $(b-h) \approx a\,n$ with some constants a, b and set $w = b - h = an$. With $h = b - w$, $n = w/a$, and $m = m_0(u)$, Eqs. (2.4)–(2.5) become

$$C\frac{\mathrm{d}u}{\mathrm{d}t} = -g_{\mathrm{Na}}[m_0(u)]^3\,(b-w)\,(u-E_{\mathrm{Na}}) - g_{\mathrm{K}}\left(\frac{w}{a}\right)^4(u-E_{\mathrm{K}}) - g_{\mathrm{L}}\,(u-E_{\mathrm{L}}) + I\,, \quad (4.3)$$

https://doi.org/10.1017/CBO9781107447615.005 Published online by Cambridge University Press

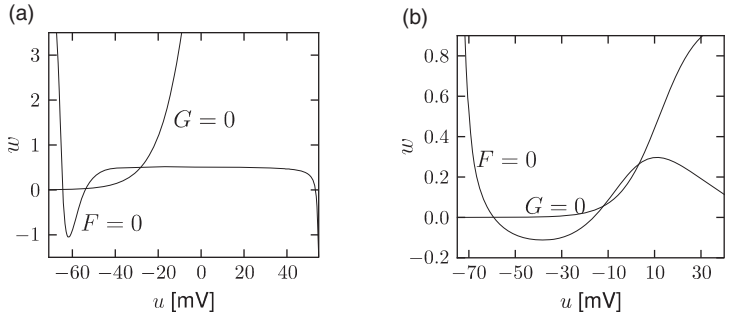

Fig. 4.3 Phase plane u, w of a Hodgkin–Huxley model reduced to two dimensions. (a) The reduction of the Hodgkin–Huxley model leads to a system of two equations, $\tau\ \mathrm{d}u/\mathrm{d}t = F(u,w) + RI$ and $\tau_w\ \mathrm{d}w/\mathrm{d}t = G(u,w)$. The ensemble of points with $F(u,w) = 0$ and $G(u,w) = 0$ is shown as a function of voltage u and recovery variable w, based on Eqs. (4.3), (4.20) and (4.21). (b) As in (a), but for the Morris–Lecar model (see text for details).

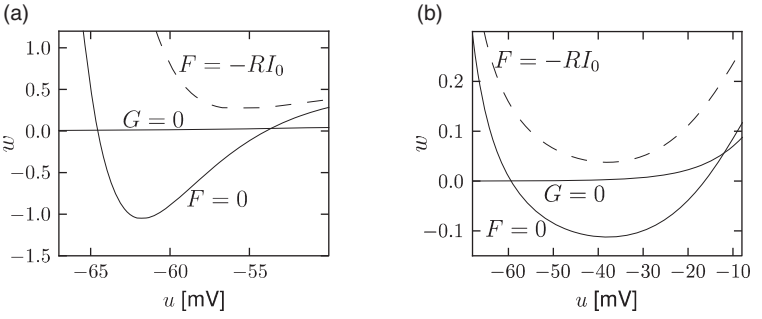

Fig. 4.4 Close-up of Fig. 4.3a and b. Solid lines: the sets of points with $F(u,w) = 0$ and $G(u,w) = 0$ are determined in the absence of stimulation ($I = 0$). Dashed line: in the presence of a constant current $I = I_0 > 0$, the set of points with $\mathrm{d}u/\mathrm{d}t = 0$ is given $F(u,w) = -RI_0$. The curve $G(u,w) = 0$ characterizing the points with $\mathrm{d}w/\mathrm{d}t = 0$ starts (for $u \to -\infty$) nearly horizontally at $w = 0$ and does not change under stimulation.

or

$$\frac{\mathrm{d}u}{\mathrm{d}t} = \frac{1}{\tau}\left[F(u,w) + RI\right], \tag{4.4}$$

with $R = g_{\mathrm{L}}^{-1}$, $\tau = RC$ and some function F. We now turn to the three equations (2.9). The m equation has disappeared since m is treated as instantaneous. Instead of the two equations (2.9) for n and h, we are left with a single effective equation

$$\frac{\mathrm{d}w}{\mathrm{d}t} = \frac{1}{\tau_w} G(u,w), \tag{4.5}$$

where τ_w is a parameter and G a function that interpolates between $\mathrm{d}n/\mathrm{d}t$ and $\mathrm{d}h/\mathrm{d}t$ (see

https://doi.org/10.1017/CBO9781107447615.005 Published online by Cambridge University Press

Section 4.2.2). Equations (4.4) and (4.5) define a general two-dimensional neuron model. If we start with the Hodgkin–Huxley model and implement the above reduction steps we arrive at functions $F(u,w)$ and $G(u,w)$ which are illustrated in Figs. 4.3a and 4.4a. The mathematical details of the reduction of the four-dimensional Hodgkin–Huxley model to the two equations (4.4) and (4.5) are given below.

Before we go through the mathematical steps, we present two examples of two-dimensional neuron dynamics which are not directly derived from the Hodgkin–Huxley model, but are attractive because of their mathematical simplicity. We will return to these examples repeatedly throughout this chapter.

Example: Morris–Lecar model

Morris and Lecar (1981) proposed a simplified two-dimensional description of neuronal spike dynamics. A first equation describes the evolution of the membrane potential u, the second equation the evolution of a slow "recovery" variable $\hat{w}$. The Morris–Lecar equations read

$$C\frac{\mathrm{d}u}{\mathrm{d}t} = -g_1\,\hat{m}_0(u)\,(u-V_1) - g_2\,\hat{w}\,(u-V_2) - g_L\,(u-V_L) + I\,, \tag{4.6}$$

$$\frac{\mathrm{d}\hat{w}}{\mathrm{d}t} = -\frac{1}{\tau(u)}\left[\hat{w} - w_0(u)\right]\,. \tag{4.7}$$

If we compare Eq. (4.6) with Eq. (4.3), we note that the first current term on the right-hand side of Eq. (4.3) has a factor $(b-w)$ which closes the channel for high voltage and which is absent in (4.6). Another difference is that neither $\hat{m}_0$ nor $\hat{w}$ in Eq. (4.6) have exponents. To clarify the relation between the two models, we could set $\hat{m}_0(u) = [m_0(u)]^3$ and $\hat{w} = (w/a)^4$. In the following we consider Eqs. (4.6) and (4.7) as a model in its own right and drop the hats over m_0 and w.

The equilibrium functions shown in Fig. 2.3a typically have a sigmoidal shape. It is reasonable to approximate the voltage dependence by

$$m_0(u) = \frac{1}{2}\left[1 + \tanh\left(\frac{u-u_1}{u_2}\right)\right], \tag{4.8}$$

$$w_0(u) = \frac{1}{2}\left[1 + \tanh\left(\frac{u-u_3}{u_4}\right)\right], \tag{4.9}$$

with parameters $u_1,\ldots,u_4$, and to approximate the time constant by

$$\tau(u) = \frac{\tau_w}{\cosh\left(\frac{u-u_3}{2u_4}\right)} \tag{4.10}$$

with a further parameter τ_w. With the above assumptions, the zero-crossings of functions $F(u,w)$ and $G(u,w)$ of the Morris–Lecar model have the shape illustrated in Fig. 4.3b.

The Morris–Lecar model (4.6)–(4.10) gives a phenomenological description of action

https://doi.org/10.1017/CBO9781107447615.005 Published online by Cambridge University Press

potentials. We shall see later on that the mathematical conditions for the firing of action potentials in the Morris–Lecar model can be discussed by phase plane analysis.

Example: FitzHugh–Nagumo model

FitzHugh and Nagumo where probably the first to propose that, for a discussion of action potential generation, the four equations of Hodgkin and Huxley can be replaced by two, i.e., Eqs. (4.4) and (4.5). They obtained sharp pulse-like oscillations reminiscent of trains of action potentials by defining the functions $F(u,w)$ and $G(u,w)$ as

$$\begin{aligned} F(u,w) &= u - \frac{1}{3}u^3 - w, \\ G(u,w) &= b_0 + b_1\, u - w\,, \end{aligned} \tag{4.11}$$

where u is the membrane voltage and w is a recovery variable (FitzHugh, 1961; Nagumo *et al*., 1962). Note that both F and G are linear in w; the sole nonlinearity is the cubic term in u. The FitzHugh–Nagumo model is one of the simplest models with non-trivial behavior lending itself to a phase plane analysis, which will be discussed below in Sections 4.3–4.5.

4.2.2 Mathematical steps (*)

The reduction of the Hodgkin–Huxley model to Eqs. (4.4) and (4.5) presented in this section is inspired by the geometrical treatment of Rinzel (1985); see also the slightly more general method of Abbott and Kepler (1990) and Kepler *et al*. (1992).

The overall aim of the approach is to replace the variables n and h in the Hodgkin–Huxley model by a single effective variable w. At each moment of time, the values $(n(t),h(t))$ can be visualized as points in the two-dimensional plane spanned by n and h; see Fig. 4.5b. We have argued above that the time course of the scaled variable an is expected to be similar to that of $b-h$. If, at each time, $an(t)$ were equal to $b-h(t)$, then all possible points (n,h) would lie on the straight line $h=b-an$ which changes through $(0,b)$ and $(1,b-a)$. It would be unreasonable to expect that all points $(n(t),h(t))$ that occur during the temporal evolution of the Hodgkin–Huxley model fall exactly on that line. Indeed, during an action potential (Fig. 4.5a), the variables $n(t)$ and $h(t)$ stay close to a straight line, but are not perfectly on it (Fig. 4.5b). The reduction of the number of variables is achieved by a projection of those points onto the line. The position along the line $h=b-a\,n$ gives the new variable w; see Fig. 4.6. The projection is the essential approximation during the reduction.

To perform the projection, we will proceed in three steps. A minimal condition for the projection is that the approximation introduces no error while the neuron is at rest. As a first step, we therefore shift the origin of the coordinate system to the rest state and introduce

https://doi.org/10.1017/CBO9781107447615.005 Published online by Cambridge University Press

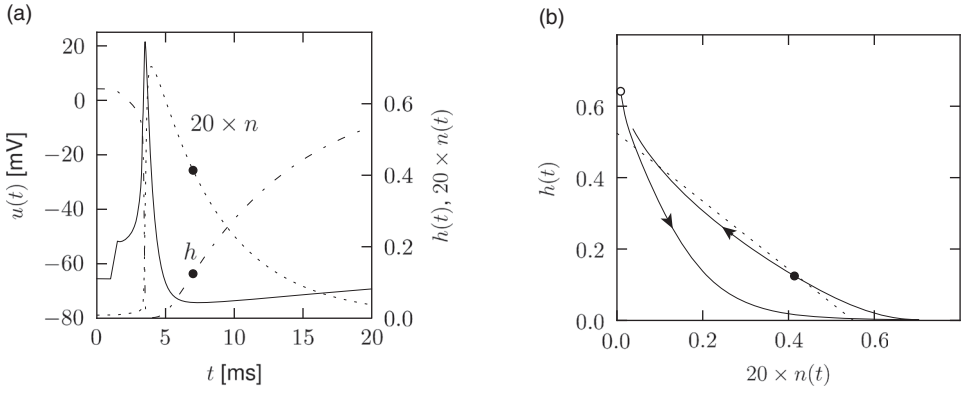

Fig. 4.5 Similarity of gating variables h and n. (a). After stimulation of the Hodgkin–Huxley model by a short current pulse, the membrane potential (solid line) exhibits an action potential. The time course of the variables n (dashed line) mirrors that of the variable h (dot-dashed). (b). During and after the action potential, the trajectory of the variables $n(t)$ and $h(t)$ (solid line) stays very close to the straight line $h = b - an$ (dashed) with slope a and offset b. The point $(n_0(u_{\text{rest}}), h_0(u_{\text{rest}}))$ is indicated with a circle.

new variables

$$x = n - n_0(u_{\text{rest}}), \tag{4.12}$$

$$y = h - h_0(u_{\text{rest}}). \tag{4.13}$$

At rest, we have $x = y = 0$.

Second, we turn the coordinate system by an angle α which is determined as follows. For a given constant voltage u, the dynamics of the gating variables n and h approaches the equilibrium values $(n_0(u), h_0(u))$. The points $(n_0(u), h_0(u))$ as a function of u define a curve in the two-dimensional plane. The slope of the curve at $u = u_{\text{rest}}$ yields the rotation angle α via

$$\tan\alpha = \frac{\frac{\mathrm{d}h_0}{\mathrm{d}u}\big|_{u_{\text{rest}}}}{\frac{\mathrm{d}n_0}{\mathrm{d}u}\big|_{u_{\text{rest}}}}. \tag{4.14}$$

Rotating the coordinate system by α turns the abscissa e_1 of the new coordinate system in a direction tangential to the curve. The coordinates (z_1, z_2) in the new system are

$$\begin{pmatrix} z_1 \\ z_2 \end{pmatrix} = \begin{pmatrix} \cos\alpha & \sin\alpha \\ -\sin\alpha & \cos\alpha \end{pmatrix} \begin{pmatrix} x \\ y \end{pmatrix}. \tag{4.15}$$

https://doi.org/10.1017/CBO9781107447615.005 Published online by Cambridge University Press

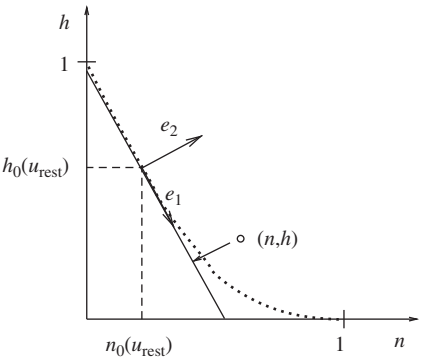

Fig. 4.6 Mathematical reduction: arbitrary points (n,h) are projected onto the line in direction of e_1 and passing through the point $(n_0(u_{\text{rest}}),h_0(u_{\text{rest}}))$. The dotted line gives the curve $(n_0(u),h_0(u))$.

Third, we set $z_2 = 0$ and retain only the coordinate z_1 along e_1. The inverse transform,

$$\begin{pmatrix} x \\ y \end{pmatrix} = \begin{pmatrix} \cos\alpha & -\sin\alpha \\ \sin\alpha & \cos\alpha \end{pmatrix} \begin{pmatrix} z_1 \\ z_2 \end{pmatrix}, \tag{4.16}$$

yields $x = z_1 \cos\alpha$ and $y = z_1 \sin\alpha$ since $z_2 = 0$. Hence, after the projection, the new values of the variables n and h are

$$n' = n_0(u_{\text{rest}}) + z_1 \cos\alpha\,, \tag{4.17}$$

$$h' = h_0(u_{\text{rest}}) + z_1 \sin\alpha\,. \tag{4.18}$$

In principle, z_1 can directly be used as the new effective variable. From (4.15) we find the differential equation

$$\frac{\mathrm{d}z_1}{\mathrm{d}t} = \cos\alpha \frac{\mathrm{d}n}{\mathrm{d}t} + \sin\alpha \frac{\mathrm{d}h}{\mathrm{d}t}\,. \tag{4.19}$$

We use Eq. (2.6) and replace, on the right-hand side, $n(t)$ and $h(t)$ by (4.17) and (4.18). The result is

$$\frac{\mathrm{d}z_1}{\mathrm{d}t} = -\cos\alpha \frac{z_1 \cos\alpha + n_0(u_{\text{rest}}) - n_0(u)}{\tau_n(u)} - \sin\alpha \frac{z_1 \sin\alpha + h_0(u_{\text{rest}}) - h_0(u)}{\tau_h(u)}\,, \tag{4.20}$$

which is of the form $\mathrm{d}z_1/\mathrm{d}t = G(u,z_1)$, as desired.

To see the relation to Eqs. (4.3) and (4.5), it is convenient to rescale z_1 and define

$$w = -\tan\alpha\, n_0(u_{\text{rest}}) - z_1 \sin\alpha\,. \tag{4.21}$$

If we introduce $a = -\tan\alpha$ and $b = a\,n_0(u_{\text{rest}}) + h_0(u_{\text{rest}})$, we find from Eq. (4.17) the variable $n' = w/a$ and from Eq. (4.18) $h' = b - w$, which are exactly the approximations that we used in (4.3). The differential equation for the variable w is of the desired form $\mathrm{d}w/\mathrm{d}t = G(u,w)$ and can be found from Eqs. (4.20) and (4.21). The resulting function $G(u,w)$ of the two-dimensional model is illustrated in Fig. 4.3a.

https://doi.org/10.1017/CBO9781107447615.005 Published online by Cambridge University Press

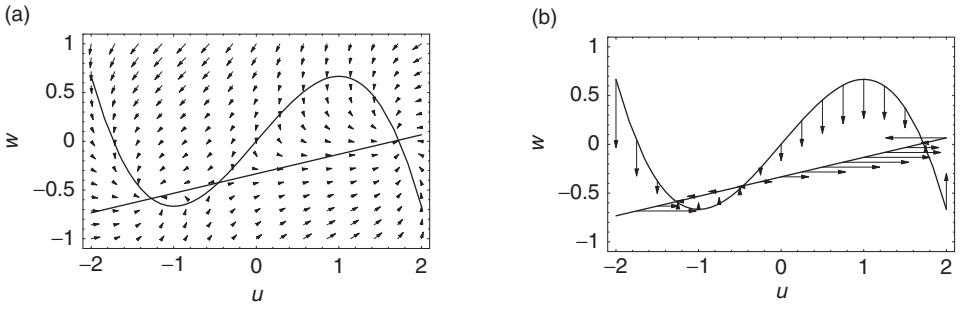

Fig. 4.7 (a) Phase portrait of the FitzHugh–Nagumo model. The u-nullcline (curved line) and the w-nullcline (straight line) intersect at the three fixed points. The direction of the arrows indicates the flow $(\dot{u},\dot{w})^T$. (b) Arrows on the u-nullcline point vertically upward or downward, while on the w-nullcline arrows are horizontal. In the neighborhood of the fixed points, arrows have a short length indicating slow movement. At the fixed point, the direction of the arrows change.

Example: Further simplification

We may further approximate the time constants τ_n and τ_h by a common function $\tau(u)$ so that the dynamics of w is

$$\frac{\mathrm{d}w}{\mathrm{d}t} = -\frac{1}{\tau(u)}\left[w - w_0(u)\right], \tag{4.22}$$

with a new equilibrium function $w_0(u)$ that is a linear combination of the functions h_0 and n_0. From Eqs. (4.20) and (4.21) we find

$$w_0(u) = -\sin\alpha\left[\cos\alpha\, n_0(u) + \sin\alpha\, h_0(u) - b\sin\alpha\right]. \tag{4.23}$$

In practice, $w_0(u)$ and $\tau(u)$ can be fitted by the expressions (4.9) and (4.10), respectively.

4.3 Phase plane analysis

In two-dimensional models, the temporal evolution of the variables $(u,w)^T$ can be visualized in the so-called phase plane. From a starting point $(u(t),w(t))^T$ the system will move in a time Δt to a new state $(u(t+\Delta t),w(t+\Delta t))^T$ which has to be determined by integration of the differential equations (4.4) and (4.5). For Δt sufficiently small, the displacement $(\Delta u,\Delta w)^T$ is in the direction of the flow $(\dot{u},\dot{w})^T$, i.e.,

$$\begin{pmatrix}\Delta u\\ \Delta w\end{pmatrix} = \begin{pmatrix}\dot{u}\\ \dot{w}\end{pmatrix}\Delta t\,, \tag{4.24}$$

https://doi.org/10.1017/CBO9781107447615.005 Published online by Cambridge University Press

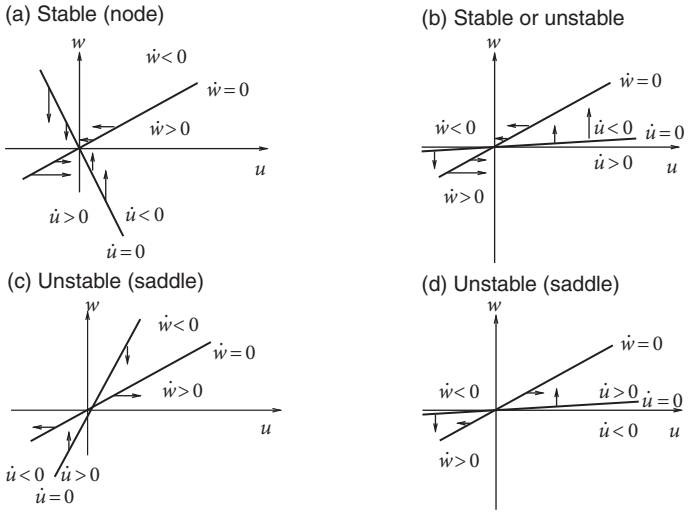

Fig. 4.8 Four examples of phase portraits around a fixed point. Case (a) is stable, cases (c) and (d) are unstable. Stability in case (b) cannot be decided with the information available from the picture alone. Cases (c) and (d) are saddle points.

which can be plotted as a vector field in the phase plane. Here $\dot{u} = \mathrm{d}u/\mathrm{d}t$ is given by (4.4) and $\dot{w} = \mathrm{d}w/\mathrm{d}t$ by (4.5). The flow field is also called the phase portrait of the system. An important tool in the construction of the phase portrait is the nullcline, which is introduced now.

4.3.1 Nullclines

Let us consider the set of points with $\dot{u} = 0$, called the u-nullcline. The direction of flow on the u-nullcline is in the direction of $(0, \dot{w})^T$, since $\dot{u} = 0$. Hence arrows in the phase portrait are vertical on the u-nullcline. Similarly, the w-nullcline is defined by the condition $\dot{w} = 0$ and arrows are horizontal. The fixed points of the system, defined by $\dot{u} = \dot{w} = 0$ are given by the intersection of the u-nullcline and the w-nullcline. In Fig. 4.7 we have three fixed points.

So far we have argued that arrows on the u-nullcline are vertical, but we do not know yet whether they point up or down. To get the extra information needed, let us return to the w-nullcline. By definition, it separates the region with $\dot{w} > 0$ from the area with $\dot{w} < 0$. Suppose we evaluate $G(u, w)$ on the right-hand side of Eq. (4.5) at a single point, e.g., at $(0, -1)$. If $G(0, -1) > 0$, then the whole area on that side of the w-nullcline has $\dot{w} > 0$. Hence, all arrows along the u-nullcline that lie on the same side of the w-nullcline

https://doi.org/10.1017/CBO9781107447615.005 Published online by Cambridge University Press

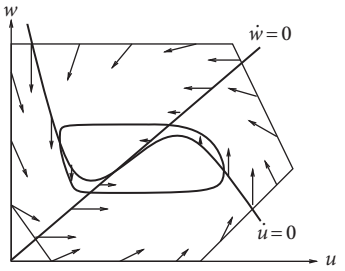

Fig. 4.9 Bounding surface around an unstable fixed point and the limit cycle (schematic figure).

as the point $(0,-1)$ point upward. The direction of arrows normally[1] changes where the nullclines intersect; see Fig. 4.7b.

4.3.2 Stability of Fixed Points

In Fig. 4.7 there are three fixed points, but which of these are stable? The local stability of a fixed point (u_{FP}, w_{FP}) is determined by linearization of the dynamics at the intersection. With $x = (u - u_{FP}, w - w_{FP})^T$, we have after the linearization

$$\frac{\mathrm{d}}{\mathrm{d}t}x = \begin{pmatrix} F_u & F_w \\ G_u & G_w \end{pmatrix} x\,, \tag{4.25}$$

where $F_u = \partial F/\partial u$, $F_w = \partial F/\partial w, \ldots$, are evaluated at the fixed point. To study the stability we set $x(t) = e\,\exp(\lambda t)$ and solve the resulting eigenvalue problem. There are two solutions with eigenvalues λ_+ and λ_- and eigenvectors e_+ and e_-, respectively. Stability of the fixed point $x = 0$ in Eq. (4.25) requires that the real part of both eigenvalues be negative. The solution of the eigenvalue problem yields $\lambda_+ + \lambda_- = F_u + G_w$ and $\lambda_+\,\lambda_- = F_u G_w - F_w G_u$. The necessary and sufficient condition for stability is therefore

$$F_u + G_w < 0 \quad \text{and} \quad F_u G_w - F_w G_u > 0\,. \tag{4.26}$$

If $F_u G_w - F_w G_u < 0$, then the imaginary part of both eigenvalues vanishes. One of the eigenvalues is positive, the other one negative. The fixed point is then called a saddle point.

Eq. (4.25) is obtained by Taylor expansion of Eqs. (4.4) and (4.5) to first order in x. If the real part of one or both eigenvalues of the matrix in Eq. (4.25) vanishes, the complete characterization of the stability properties of the fixed point requires an extension of the Taylor expansion to higher order.

[1]Exceptions are the rare cases where the function F or G is degenerate: for example, $F(u,w) = w^2$.

https://doi.org/10.1017/CBO9781107447615.005 Published online by Cambridge University Press

Example: Linear model

Let us consider the linear dynamics

$$\begin{aligned} \dot{u} &= a\,u - w, \\ \dot{w} &= \varepsilon\,(b\,u - w)\,, \end{aligned} \tag{4.27}$$

with positive constants $b, \varepsilon > 0$. The u-nullcline is $w = a\,u$, the w-nullcline is $w = b\,u$. For the moment we assume $a < 0$. The phase diagram is that of Fig. 4.8a. Note that by decreasing the parameter ε, we may slow down the w-dynamics in Eq. (4.27) without changing the nullclines.

Because $F_u + G_w = a - \varepsilon < 0$ for $a < 0$ and $F_u G_w - F_w G_u = \varepsilon\,(b - a) > 0$, it follows from (4.26) that the fixed point is stable. Note that the phase portrait around the left fixed point in Fig. 4.7 has locally the same structure as the portrait in Fig. 4.8a. We conclude that the left fixed point in Fig. 4.7 is stable.

Let us now keep the w-nullcline fixed and turn the u-nullcline by increasing a to positive values; see Fig. 4.8b and c. Stability is lost if $a > \min\{\varepsilon, b\}$. Stability of the fixed point in Fig. 4.8b can therefore not be decided without knowing the value of ε. On the other hand, in Fig. 4.8c we have $a > b$ and hence $F_u G_w - F_w G_u = \varepsilon\,(b - a) < 0$. In this case one of the eigenvalues is positive ($\lambda_+ > 0$) and the other one negative ($\lambda_- < 0$), hence we have a saddle point. The imaginary parts of the eigenvalues vanish. The eigenvectors e_- and e_+ are therefore real and can be visualized in the phase space. A trajectory through the fixed point in the direction of e_- is attracted toward the fixed point. This is, however, the only direction by which a trajectory may reach the fixed point. Any small perturbation around the fixed point which is not strictly in the direction of e_2 will grow exponentially. A saddle point as in Fig. 4.8c plays an important role in so-called type I neuron models that will be introduced in Section 4.4.1.

For the sake of completeness we also study the linear system

$$\begin{aligned} \dot{u} &= -a\,u + w, \\ \dot{w} &= \varepsilon\,(b\,u - w)\,, \text{ with } 0 < a < b\,, \end{aligned} \tag{4.28}$$

with positive constants a, b, and ε. This system is identical to Eq. (4.27) except that the sign of the first equation is flipped. As before we have nullclines $w = a\,u$ and $w = b\,u$; see Fig. 4.8d. Note that the nullclines are identical to those in Fig. 4.8b, only the direction of the horizontal arrows on the w-nullcline has changed.

Since $F_u G_w - F_w G_u = \varepsilon\,(a - b)$, the fixed point is unstable if $a < b$. In this case, the imaginary part of the eigenvalues vanish and one of the eigenvalues is positive ($\lambda_+ > 0$) while the other one is negative ($\lambda_- < 0$). Thus the fixed point can be classified as a saddle point.

One of the attractive features of phase plane analysis is that there is a direct method to show the existence of limit cycles. The theorem of Poincaré–Bendixson (Hale and

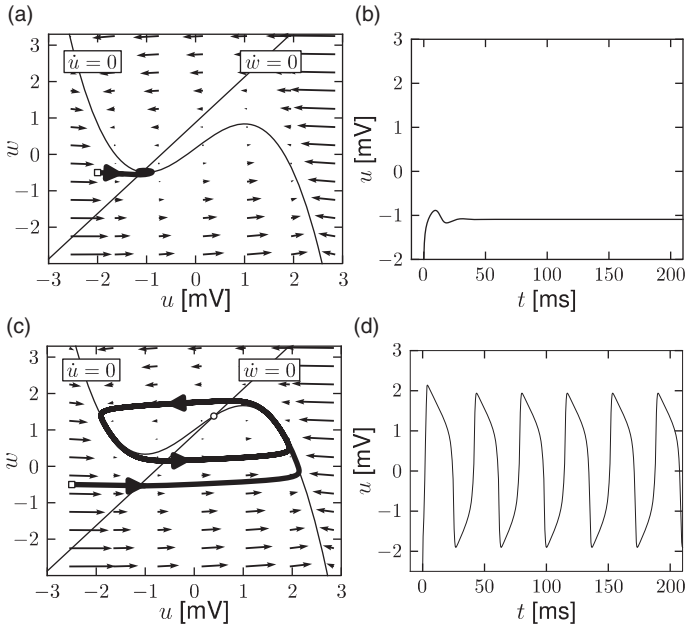

Fig. 4.10 (a) The nullclines of the FitzHugh–Nagumo model for zero input. The thin curved line is the u-nullcline; the w-nullcline is the straight line, $w = b_0 + b_1 u$, with $b_0 = 0.9, b_1 = 1.0$. The thick line is a trajectory that starts at $(-2, -0.5)$ (open square) and converges to the fixed point at $(-1.1, -0.5)$. (b) Time course of the membrane potential of the trajectory shown in (a). (c) Same as in (a) but with positive input $I = 2$ so that the fixed point in (a) is replaced by a limit cycle (thick line). (d) Voltage time course of the trajectory shown in (c). Trajectories are the result of numerical integration of Eqs. (4.29) and (4.30) with $\varepsilon = 1.25$.

Koçac, 1991) tells us that, if (i) we can construct a bounding surface around a fixed point so that all flux arrows on the surface are pointing toward the interior, and (ii) the fixed point in the interior is repulsive (real part of both eigenvalues positive), then there must exist a stable limit cycle around that fixed point.

The proof follows from the uniqueness of solutions of differential equations, which implies that trajectories cannot cross each other. If all trajectories are pushed away from the fixed point, but cannot leave the bounded surface, then they must finally settle on a limit cycle; see Fig. 4.9. Note that this argument holds only in two dimensions.

In dimensionless variables the FitzHugh–Nagumo model is

$$\frac{\mathrm{d}u}{\mathrm{d}t} = u - \frac{1}{3}u^3 - w + I, \tag{4.29}$$

$$\frac{\mathrm{d}w}{\mathrm{d}t} = \varepsilon\,(b_0 + b_1\,u - w)\,. \tag{4.30}$$

https://doi.org/10.1017/CBO9781107447615.005 Published online by Cambridge University Press

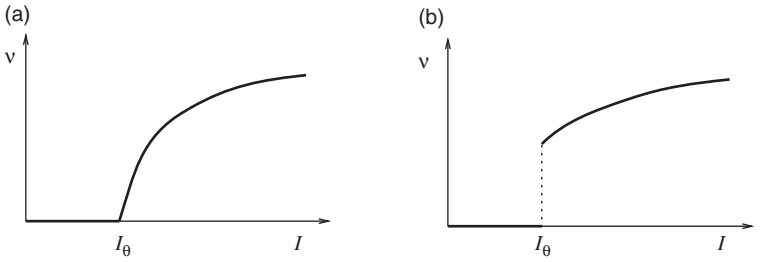

Fig. 4.11 (a) Gain function for models of type I. The frequency ν during a limit cycle oscillation is a continuous function of the applied current I. (b) The gain function of type II models has a discontinuity.

Time is measured in units of τ, and $\varepsilon = \tau/\tau_w$ is the ratio of the two time scales. The u-nullcline is $w = u - u^3/3 + I$ with maxima at $u = \pm 1$. The maximal slope of the u-nullcline is $\mathrm{d}w/\mathrm{d}u = 1$ at $u = 0$; for $I = 0$ the u-nullcline has zeros at 0 and $\pm\sqrt{3}$. For $I \neq 0$ the u-nullcline is shifted vertically. The w-nullcline is a straight line $w = b_0 + b_1 u$. For $b_1 > 1$, there is always exactly one intersection, for any I. The two nullclines are shown in Fig. 4.10.

A comparison of Fig. 4.10a with the phase portrait of Fig. 4.8a, shows that the fixed point is stable for $I = 0$. If we increase I the intersection of the nullclines moves to the right; see Fig. 4.10c. According to the calculation associated with Fig. 4.8b, the fixed point loses stability as soon as the slope of the u-nullcline becomes larger than ε. It is possible to construct a bounding surface around the unstable fixed point so that we know from the Poincaré–Bendixson theorem that a limit cycle must exist. Figures 4.10a and 4.10c show two trajectories, one for $I = 0$ converging to the fixed point and another one for $I = 2$ converging toward the limit cycle. The horizontal phases of the limit cycle correspond to a rapid change of the voltage, which results in voltage pulses similar to a train of action potentials; see Fig. 4.10d.

4.4 Type I and type II neuron models

We have already seen in Chapter 2 that neuron models fall into two classes: those with a continuous frequency–current curve are called type I whereas those with a discontinuous frequency–current curve are called type II. The characteristic curves for both model types are illustrated in Fig. 4.11. The onset of repetitive firing under constant current injection is characterized by a minimal current I_θ, also called the rheobase current.

For two-dimensional neuron models, the firing behavior of both neuron types can be understood by phase plane analysis. To do so we need to observe the changes in structure and stability of fixed points when the current passes from a value below I_θ to a value just above I_θ, where I_θ determines the onset of repetitive firing. Mathematically speaking, the point I_θ where the transition in the number or stability of fixed points occurs is called a bifurcation point and I is the bifurcation parameter.

https://doi.org/10.1017/CBO9781107447615.005 Published online by Cambridge University Press

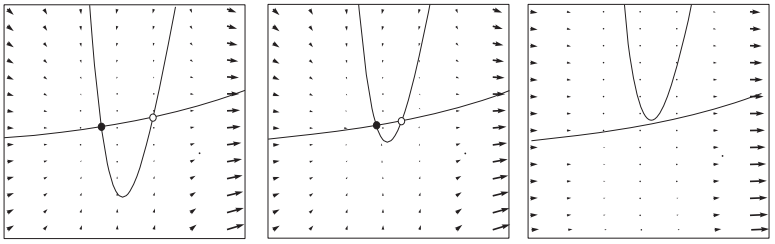

Fig. 4.12 Saddle-node bifurcation. The u-nullcline is represented as a parabola that moves upward as the current is increased (from left to right). The saddle point is shown as an open circle and the node as a filled circle. When the current is increased, the two fixed points, which are initially far apart (left), move closer together (middle) and finally annihilate (right).

Example: Number of fixed points changes at bifurcation

Let us recall that the fixed points of the system lie at the intersection of the u-nullcline with the w-nullcline. Fig. 4.3 shows examples of two-dimensional neuron models where the u-nullcline crosses the w-nullclines three times so that the models exhibit three fixed points. If the external driving current I is slowly increased, the u-nullcline shifts vertically upward.[2] If the driving current I becomes strong enough, the two left-most fixed points merge and disappear; see Fig. 4.4. The moment when the two fixed points disappear is the bifurcation point. At this point a qualitative change in the dynamics of the neuron model is observed, e.g., the transition from the resting state to periodic firing. These changes are discussed in the following subsections.

4.4.1 Type I models and saddle-node-onto-limit-cycle bifurcation

Neuron models with a continuous gain function are called type I. Mathematically, a saddle-node-onto-limit-cycle bifurcation generically gives rise to a type I behavior, as we will explain now.

For zero input and weakly positive input, we suppose that our neuron model has three fixed points in a configuration such as that in Fig. 4.13: a stable fixed point (node) to the left, a saddle point in the middle, and an unstable fixed point to the right. If I is increased, the u-nullcline moves upward and the stable fixed point merges with the saddle and disappears (Fig. 4.12). We are left with the unstable fixed point around which there must be a limit cycle provided the flux is bounded. If the limit cycle passes through the region where the saddle and node disappeared, the scenario is called a saddle-node-onto-limit-cycle bifurcation.

Can we say anything about the frequency of the limit cycle? Just before the transition point where the two fixed points merge, the system exhibits a stable fixed point which (locally) attracts trajectories. As a trajectory gets close to the stable fixed point, its velocity

[1] It may also undergo some changes in shape, but these are not relevant for the following discussion.

https://doi.org/10.1017/CBO9781107447615.005 Published online by Cambridge University Press

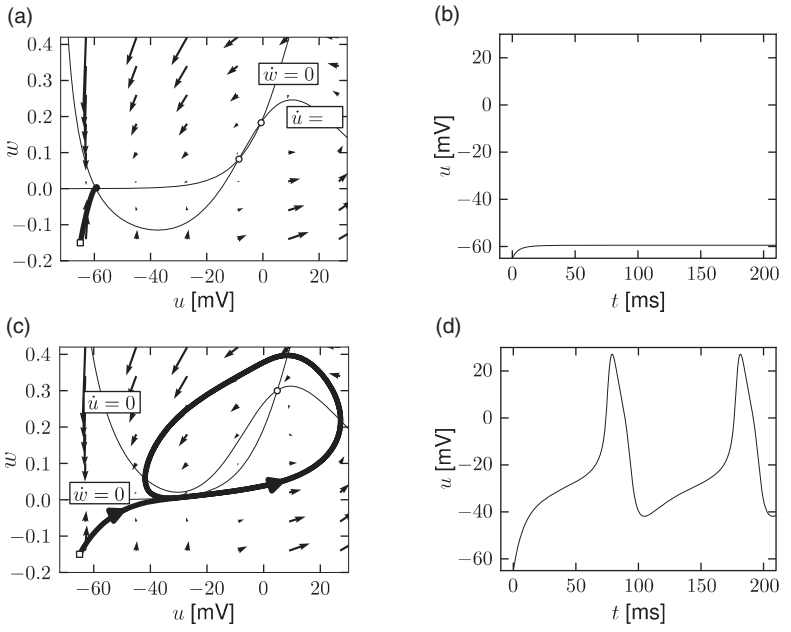

Fig. 4.13 (a) The nullclines of the Morris–Lecar model for zero input. The w-nullcline is flat at low u but increases monotonically above $u = -20$, the u-nullcline is the nonlinear curve crossing the w-nullcline in three points. (a) Trajectory starting at $(-65,-0.15)$ (open square) converges to the stable fixed point at (-59,0) (filled circle). (b) Time course of the membrane potential of the trajectory shown in (a). (c) Same as in (a) but with positive input $I = 45$. The stable fixed point in (a) has merged with the saddle (open circle in (a)) and disappeared leaving a limit cycle around the third, unstable, fixed point. (d) Voltage time course of the trajectory shown in (c). Trajectories are the results of numerical integration of Eqs. (4.6)–(4.10).

decreases until it finally stops at the fixed point. Let us now consider the situation where the driving current is a bit larger so that $I = I_\theta$. This is the transition point, where the two fixed points merge and a new limit cycle appears. At the transition point the limit cycle has zero frequency because it passes through the two merging fixed points where the velocity of the trajectory is zero. If I is increased a little, the limit cycle still "feels" the "ghost" of the disappeared fixed points in the sense that the velocity of the trajectory in that region is very low. While the fixed points have disappeared, the "ruins" of the fixed points are still present in the phase plane. Thus the onset of oscillation is continuous and occurs with zero frequency. Models which fall into this class are therefore of type I; see Fig. 4.11.

From the above discussion it should be clear that, if we increase I, we encounter a transition point where two fixed points disappear, namely, the saddle and the stable fixed point (node). At the same time a limit cycle appears. If we come from the other side, we have first a limit cycle which disappears at the moment when the saddle-node pair shows up. The transition is therefore called a saddle-node bifurcation on a limit cycle.

https://doi.org/10.1017/CBO9781107447615.005 Published online by Cambridge University Press

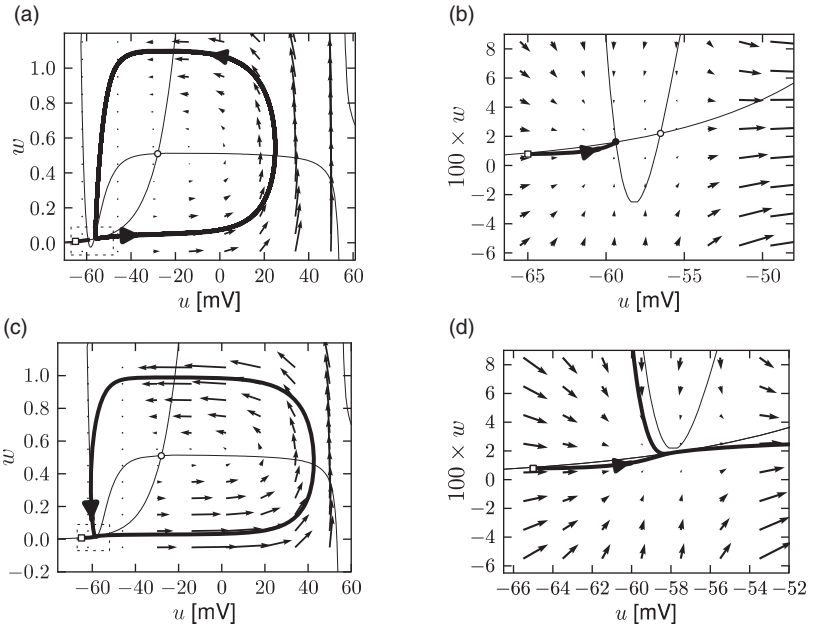

Fig. 4.14 Reduced Hodgkin–Huxley model with nullclines and dynamics of a type I model. (a) For weakly positive input, the u-nullcline has three intersections with the w-nullcline. (b) Zoom onto the two left-most fixed points. A trajectory (thick solid line) is attracted toward the left fixed point. (c) For input $I > I_\theta$, the u-nullcline is shifted vertically and only one fixed point remains which is unstable. The trajectory starting from the same initial condition as in (a) turns into a limit cycle. (d) Zoom onto the same region as in (b). The limit cycle passes through the region where the two fixed points have been before, but these fixed points have now disappeared. The nearly vanishing length of the arrows indicates that movement of the trajectory in this region is very slow giving rise to a near-zero firing frequency.

Example: Morris–Lecar model

Depending on the choice of parameters, the Morris–Lecar model is of either type I or type II. We consider a parameter set where the Morris–Lecar model has three fixed points located such that two of them lie in the unstable region where the u-nullcline has large positive slope as indicated schematically in Fig. 4.13. Comparison of the phase portrait of Fig. 4.13 with that of see Fig. 4.8 shows that the left fixed point is stable as in Fig. 4.8a, the middle one is a saddle point as in Fig. 4.8c, and the right one is unstable as in Fig. 4.8b provided that the slope of the u-nullcline is sufficiently positive. Thus we have the sequence of three fixed points necessary for a saddle-node-onto-limit-cycle bifurcation.

https://doi.org/10.1017/CBO9781107447615.005 Published online by Cambridge University Press

Example: Hodgkin–Huxley model reduced to two dimensions

The reduced Hodgkin–Huxley model of Fig. 4.3a has three fixed points. Stability analysis of the fixed points or comparison of the phase portrait of this model in Fig. 4.14a with the standard cases in Fig. 4.8 shows that the left fixed point is stable, the middle one is a saddle, and the right one is unstable. If a step current I is applied, the u-nullcline undergoes some minor changes in shape, but mainly shifts upward. If the step is big enough, two of the fixed points disappear. The resulting limit cycle passes through the ruins of the fixed point; see Figs. 4.14c and 4.14d.

4.4.2 Type II models and saddle-node-off-limit-cycle bifurcation

There is no fundamental reason why a limit cycle should appear at a saddle-node bifurcation. Indeed, in one-dimensional differential equations, saddle-node bifurcations are possible, but never lead to a limit cycle. Moreover, if a limit cycle exists in a two-dimensional system, there is no reason why it should appear directly at the bifurcation point – it can also exist before the bifurcation point is reached. In this case, the limit cycle does not pass through the ruins of the fixed point and therefore has finite frequency. This gives rise to a type II neuron model. The corresponding bifurcation can be classified as saddle-node-off-limit-cycle.

Example: Hodgkin–Huxley model reduced to two dimensions

Fig. 4.15 shows the same neuron model as Fig. 4.14 except for one single change in parameter: the time scale τ_w in Eq. (4.5) for the w-dynamics is slightly faster. While the position and shape of the nullclines is unchanged, the dynamics are different.

To understand the difference we focus on Fig. 4.15d. The limit cycle triggered by a current step does not touch the region where the ruins of the fixed points lie, but passes further to the right. Thus the bifurcation is of the type saddle-node-off-limit-cycle, the limit cycle has finite frequency, and the neuron model is of type II.

Example: Saddle-node without limit cycle

Not all saddle-node bifurcations lead to a limit cycle. If the slope of the w-nullcline of the FitzHugh–Nagumo model defined in Eqs. (4.29) and (4.30) is smaller than 1, it is possible to have three fixed points, one of them unstable and the other two stable; see Fig. 4.7. The system is therefore bistable. If a positive current $I > 0$ is applied the u-nullcline moves upward. Eventually the left stable fixed point and the saddle merge and disappear via a (simple) saddle-node bifurcation. Since the right fixed point remains stable, no oscillation occurs.

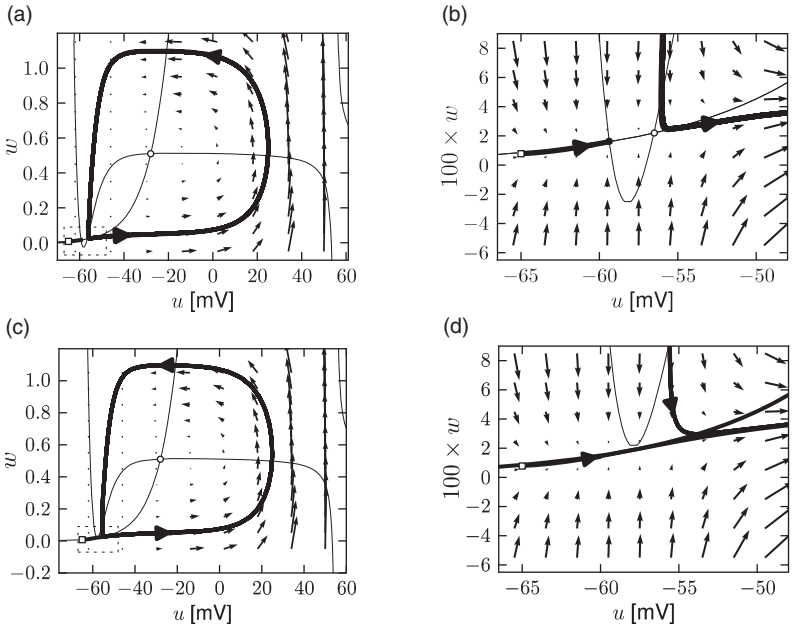

Fig. 4.15 Reduced Hodgkin–Huxley model with nullclines and dynamics of a type II model. (a) For weakly positive input, the u-nullcline (solid line) has three intersections with the w-nullcline (dashed line). (b) Zoom onto the two left-most fixed points. A trajectory (thick solid line) is attracted toward the left fixed point. (c) For input $I > I_\theta$, only one fixed point remains which is unstable. The trajectory starting from the same initial condition as in A turns into a limit cycle. (d) Zoom onto the same region as in (b). The limit cycle passes to the right of the region where the two fixed points have been in (b). Arrows along the limit cycle indicate finite speed of the trajectory, so that the limit cycle has a nonzero firing frequency.

4.4.3 Type II models and Hopf bifurcation

The typical jump from zero to a finite firing frequency, observed in the frequency–current curve of type II models can arise by different bifurcation types. One important example is a Hopf bifurcation.

Let us recall that the fixed points of the system lie at the intersection of the u-nullcline with the w-nullcline. In the FitzHugh–Nagumo model, with parameters as in Fig. 4.10, there is always a single fixed point whatever the (constant) driving current I. Nevertheless, while I is slowly increased, the behavior of the system changes qualitatively from a stable fixed point to a limit cycle; see Fig. 4.10. The transition occurs when the fixed point loses its stability.

From the solution of the stability problem in Eq. (4.25) we know that the eigenvalues $\lambda_{+/-}$ form a complex conjugate pair with a real part γ and a imaginary part $+/-\omega$

https://doi.org/10.1017/CBO9781107447615.005 Published online by Cambridge University Press

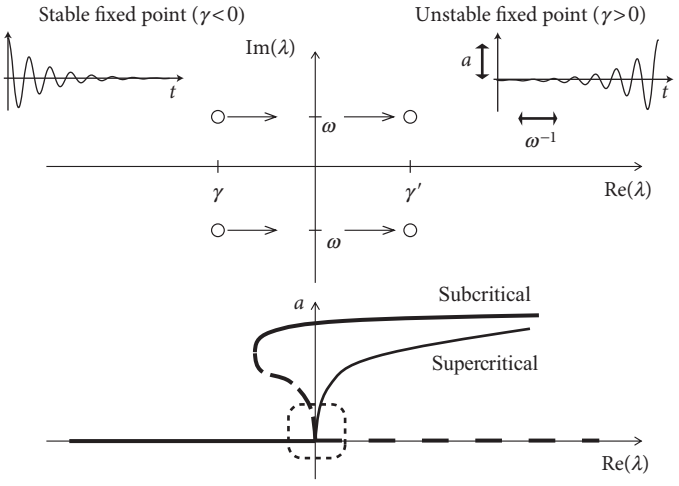

Fig. 4.16 Hopf bifurcation. Top: Complex plane of eigenvalues. When the bifurcation parameter increases, the real part of the complex eigenvalues $\lambda_{+/-} = \gamma \pm i\,\omega$ passes at the bifurcation point from a negative value ($\gamma < 0$) to a positive one. Associated stable and unstable oscillatory solutions are shown in left and right insets, respectively. Bottom: Amplitude a of oscillatory solutions as a function of γ. For $\gamma < 0$ the fixed point (constant solution) is stable corresponding to an oscillation of zero amplitude. At the bifurcation point, the constant solution loses its stability (dashed line) and a novel oscillatory solution appears. The amplitude of the oscillatory solution increases continuously. For a supercritical Hopf bifurcation the oscillatory solution is stable (solid line) whereas for a subcritical Hopf bifurcation, it is unstable close to the bifurcation point. The linear bifurcation analysis is valid only in the direct neighborhood of the bifurcation point (dashed box) and cannot predict the stable limit cycle (solid line) of the subcritical Hopf bifurcation.

(Fig. 4.16). The fixed point is stable if $\gamma < 0$. At the transition point, the real part vanishes and the eigenvalues are

$$\lambda_{\pm} = \pm i\sqrt{F_u G_w - G_u F_w}\,. \tag{4.31}$$

These eigenvalues correspond to an oscillatory solution (of the linearized equation) with a frequency given by $\omega = \sqrt{F_u G_w - G_u F_w}$. The above scenario of stability loss in combination with an emerging oscillation is called a Hopf bifurcation.

Unfortunately, the discussion so far does not tell us anything about the stability of the oscillatory solution. If the new oscillatory solution, which appears at the Hopf bifurcation, is itself unstable (which is more difficult to show), the scenario is called a subcritical Hopf bifurcation (Fig. 4.16). This is the case in the FitzHugh–Nagumo model where, owing to the instability of the oscillatory solution in the neighborhood of the Hopf bifurcation, the system blows up and approaches another limit cycle of large amplitude; see Fig. 4.10. The stable large-amplitude limit cycle solution exists, in fact, slightly before I reaches the

critical value of the Hopf bifurcation. Thus there is a small regime of bistability between the fixed point and the limit cycle.

In a supercritical Hopf bifurcation, on the other hand, the new periodic solution is stable. In this case, the limit cycle would have a small amplitude if I is just above the bifurcation point. The amplitude of the oscillation grows with the stimulation I (Fig. 4.16). Such periodic oscillations of small amplitude are not linked to neuronal firing, but must rather be interpreted as spontaneous subthreshold oscillations.

Whenever we have a Hopf bifurcation, be it subcritical or supercritical, the limit cycle starts with finite frequency. Thus if we plot the frequency of the oscillation in the limit cycle as a function of the (constant) input I, we find a discontinuity at the bifurcation point. However, only models with a subcritical Hopf bifurcation give rise to large-amplitude oscillations close to the bifurcation point. We conclude that models where the onset of oscillations occurs via a subcritical Hopf bifurcation exhibit a gain function of type II.

Example: FitzHugh–Nagumo model

The appearance of oscillations in the FitzHugh–Nagumo Model discussed above in Fig. 4.10 is of type II. If the slope of the w-nullcline is larger than 1, there is only one fixed point, whatever I. With increasing current I, the fixed point moves to the right. Eventually it loses stability via a Hopf bifurcation.

4.5 Threshold and excitability

We have seen in Section 4.1 that the Hodgkin–Huxley model does not have a clear-cut firing threshold. Nevertheless, there is a critical regime where the sensitivity to input current pulses is so high that it can be fairly well approximated by a threshold. For weak stimuli, the voltage trace returns more or less directly to the resting potentials. For stronger stimuli it makes a large detour, that is, the model emits a spike; see Fig. 4.1b. This property is characteristic for a large class of systems collectively termed *excitable systems*.

For two-dimensional models, excitability can be discussed in phase space in a transparent manner. We pose the following questions. What are the conditions for a threshold behavior? If there is no sharp threshold, what are the conditions for a regime of high (threshold-like) sensitivity? As we have seen in Section 4.1, the search for a threshold yields different results for step or pulsatile currents. We shall see now that, for stimulation with a short current pulse of variable amplitude, models with saddle-node bifurcation (on or off a limit cycle) indeed have a threshold, whereas models where firing arises via a Hopf bifurcation have not. On the other hand, even models with Hopf bifurcation can show threshold-like behavior for current pulses if the dynamics of w are considerably slower than that of u.

Throughout this section we use the following stimulation paradigm. We assume that the neuron is at rest (or in a known state) and apply a short current pulse $I(t) = q\,\delta(t)$

https://doi.org/10.1017/CBO9781107447615.005 Published online by Cambridge University Press

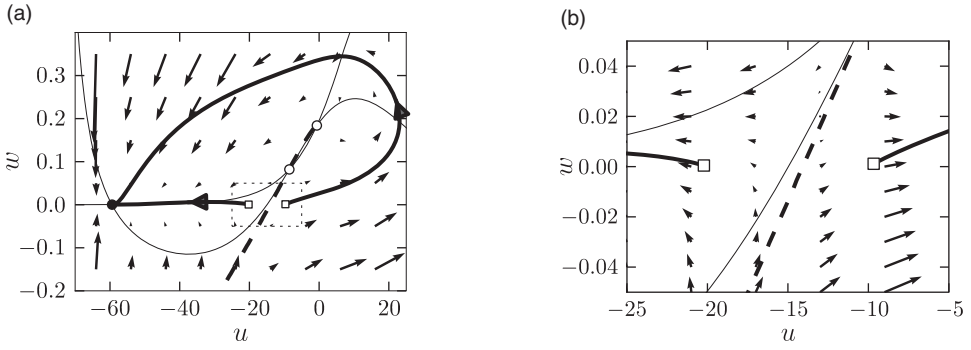

Fig. 4.17 Threshold in a type I model. (a) The stable manifold (thick dashed line) acts as a threshold. Trajectories (thick solid lines) that start to the right of the stable manifold cannot return directly to the stable fixed point (filled circle) but have to take a detour around the repulsive fixed point (circle at $(u,w) \approx (-1, 0.2)$). The result is a spike-like excursion of the u-variable. Thin lines are the nullclines. (b) Blow-up of the rectangular region in (a). The starting points of the two sample trajectories are marked by squares.

of amplitude $q > 0$. The input pulse influences the neuronal dynamics via Eq. (4.4). As a consequence, the voltage u jumps at $t = 0$ by an amount $\Delta u = qR/\tau$; see Eq. (4.4). With $\tau = RC$ the voltage jump can be written $\Delta u = q/C$ in agreement with the discussion in Section 4.1.1.

Since the current pulse does not act directly on the recovery variable w (see Eq. (4.5)), the time course of $w(t)$ is continuous. In the phase plane, the current pulse therefore shifts the value of state variables (u,w) of the system *horizontally* to a new value $(u+\Delta u, w)$. How does the system return to equilibrium? How does the behavior depend on the amplitude q of the current pulse?

We will see that the behavior can depend on the charge q of the current pulse in two qualitatively distinct ways. In type I models, the response to the input shows an "all-or-nothing" behavior and consists of either a significant pulse (that is, an action potential) or a simple decay back to rest. To this effect, type I models exhibit a threshold behavior. If the action potential occurs, it has always roughly the same amplitude, but occurs at different delays depending on the strength q of the stimulating current pulse. In models with a Hopf bifurcation, on the other hand, the amplitude of the response depends continuously on the amplitude q. Therefore, models with a Hopf bifurcation do not have a sharp threshold. Type II models with a saddle-node-off-limit-cycle bifurcation have a threshold behavior for pulse injection similar to that of type I models.

Example: Single current pulses versus multiple pulses

The discussion so far has been focused on an isolated current pulse of charge q. Note, however, that even in a model with threshold, a first input pulse that lifts the state of the system above the threshold can be counterbalanced by a second negative input which

https://doi.org/10.1017/CBO9781107447615.005 Published online by Cambridge University Press

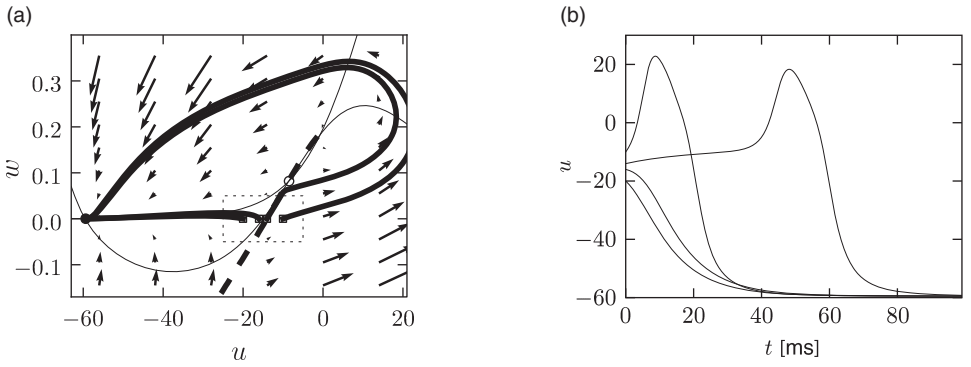

Fig. 4.18 Type I model and delayed spike initiation. (a) Trajectories in the phase starting with initial conditions (u_0, w_{rest}) where $u_0 = -20, -17, -14, -10$ are close to the threshold. (b) Projection of the trajectories on the voltage axis. Close to the threshold, spike initiation starts with a delay, but the amplitude of the action potential is always roughly the same.

pulls the state of the system back. Thus, even in models with a threshold, the threshold is only "seen" for the specific input scenario considered here, namely, one isolated short current pulse.

4.5.1 Type I models

As discussed above, type I models are characterized by a set of three fixed points, a stable one to the left, a saddle point in the middle, and an unstable one to the right. The linear stability analysis at the saddle point reveals, by definition of a saddle, one positive and one negative eigenvalue, λ_+ and λ_-, respectively. The imaginary parts of the eigenvalues vanish. Associated with λ_- is the (real) eigenvector e_-. A trajectory which approaches the saddle in the direction of e_- from either side will eventually converge toward the fixed point. There are two of these trajectories. The first one starts at infinity and approaches the saddle from below. In the case of a type I mode, the second one starts at the unstable fixed point and approaches the saddle from above. The two together define the stable manifold of the fixed point (Hale and Koçac, 1991). A perturbation around the fixed point that lies on the stable manifold returns to the fixed point. All other perturbations will grow exponentially.

The stable manifold plays an important role for the excitability of the system. Due to the uniqueness of solutions of differential equations, trajectories cannot cross. This implies that all trajectories with initial conditions to the right of the stable manifold must make a detour around the unstable fixed point before they can reach the stable fixed point. Trajectories with initial conditions to the left of the stable manifold return immediately toward the stable fixed point; see Fig. 4.17.

Let us now apply these considerations to neuron models driven by a short current pulse. At rest, the neuron model is at the stable fixed point. A short input current pulse moves the

https://doi.org/10.1017/CBO9781107447615.005 Published online by Cambridge University Press

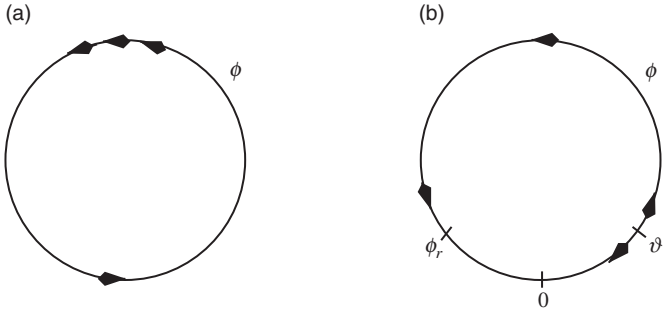

Fig. 4.19 Type I model as a phase model. (a) For $I > 0$, the system is on a limit cycle. The phase velocity $\mathrm{d}\phi/\mathrm{d}t$ is positive everywhere. (b) For $I < 0$, the phase has a stable fixed point at $\phi = \phi_r$ and an unstable fixed point at $\phi = \vartheta$.

state of the system to the right. If the current pulse is small, the new state of the system is to the left of the stable manifold. Hence the membrane potential u decays back to rest. If the current pulse is sufficiently strong, it will shift the state of the system to the right of the stable manifold. Since the resting point is the only stable fixed point, the neuron model will eventually return to the resting potential. To do so, it has, however, to take a large detour which is seen as a pulse in the voltage variable u. The stable manifold thus acts as a threshold for spike initiation, if the neuron model is probed with an isolated current pulse.

Example: Delayed spike initiation

We consider a sequence of current pulse of variable amplitude that cause a jump to initial values (u_0, w_{rest}) where u_0 is close to the firing threshold identified above. As u_0 approaches the firing threshold from above, action potentials are elicited with increasing delay; see Fig. 4.18b. The reason is that close to the firing threshold (i.e., the stable manifold of the saddle point) the trajectory is attracted toward the saddle point without reaching it. At the saddle point, the velocity of the trajectory would be zero. Close to the saddle point the velocity of the trajectory is nonzero, but extremely slow. The rapid rise of the action potential only starts after the trajectory has gained a minimal distance from the saddle point.

Example: Canonical type I model

We have seen in the previous example that, for various current amplitudes, the trajectory always takes nearly the same path on its detour in the two-dimensional phase plane. Let us therefore simplify further and just describe the position or "phase" on this standard path.

https://doi.org/10.1017/CBO9781107447615.005 Published online by Cambridge University Press

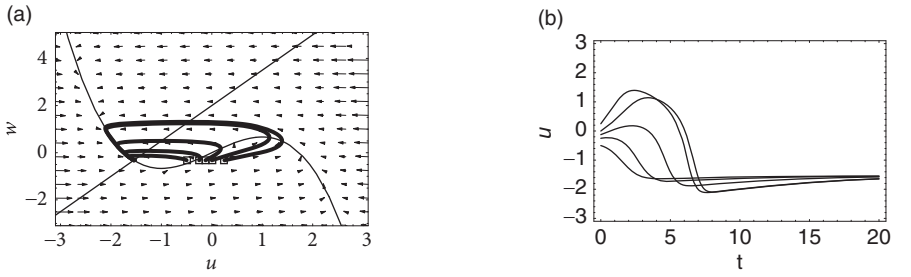

Fig. 4.20 Threshold behavior in a model with Hopf bifurcation. (a) Trajectories in the phase starting with initial conditions (u_0, w_{rest}) where $u_0 = -0.5, -0.25, -0.125, 0, 0.25$. (b) Projection of the trajectories on the voltage axis. For $u_0 \leq -0.25$, the trajectories return rapidly to rest. The trajectories with $u_0 \geq -0.125$ start with positive slope. Parameters were $b_0 = 2$, $b_1 = 1.5$, $\varepsilon = 0.1$ with $I = 0$.

Consider the one-dimensional model

$$\frac{\mathrm{d}\phi}{\mathrm{d}t} = q\,(1-\cos\phi) + I\,(1+\cos\phi) \tag{4.32}$$

where $q > 0$ is a parameter and I is the applied current, with $0 < |I| < q$. The variable ϕ is the phase along the limit cycle trajectory. Formally, a spike is said to occur whenever $\phi = \pi$.

For $I < 0$ on the right-hand side of Eq. (4.32), the phase equation $\mathrm{d}\phi/\mathrm{d}t$ has two fixed points. The resting state is at the stable fixed point $\phi = \phi_r$. The unstable fixed point at $\phi = \vartheta$ acts as a threshold; see Fig. 4.19b. Let us now assume initial conditions slightly above threshold, namely, $\phi_0 = \vartheta + \delta\phi$. Since $\mathrm{d}\phi/\mathrm{d}t|_{\phi_0} > 0$ the system starts to fire an action potential but for $\delta\phi \ll 1$ the phase velocity is still close to zero and the maximum of the spike (corresponding to $\phi = \pi$) is reached only after a long delay. This delay depends critically on the initial condition.

For all currents $I > 0$, we have $\mathrm{d}\phi/\mathrm{d}t > 0$, so that the system is circling along the limit cycle; see Fig. 4.19a. The minimal velocity is $\mathrm{d}\phi/\mathrm{d}t = I$ for $\phi = 0$. The period of the limit cycle can be found by integration of (4.32) around a full cycle. Let us now reduce the amplitude of the applied current I. For $I \to 0$, the velocity along the trajectory around $\phi = 0$ tends to zero. The period of one cycle $T(I)$ therefore tends to infinity. In other words, for $I \to 0$, the frequency of the oscillation $\nu = 1/T(I)$ decreases (continuously) to zero, the characteristic feature of type I models.

The model (4.32) is a canonical model in the sense that all type I neuron models close to the point of a saddle-node-on-limit-cycle bifurcation can be mapped onto Eq. (4.32) (Ermentrout, 1996).

4.5.2 Hopf bifurcations

In contrast to models with saddle-node bifurcation, a neuron model with a Hopf bifurcation does not have a stable manifold and, hence, there is no "forbidden line" that acts as a

https://doi.org/10.1017/CBO9781107447615.005 Published online by Cambridge University Press

sharp threshold. Instead of the typical all-or-nothing behavior of type I models there is a continuum of trajectories; see Fig. 4.20a.

Nevertheless, if the time scale of the u-dynamics is much faster than that of the w-dynamics, then there is a critical regime where the sensitivity to the amplitude of the input current pulse can be extremely high. If the amplitude of the input pulse is increased by a tiny amount, the amplitude of the response increases a lot. In practice, the consequences of the regime of high sensitivity are similar to that of a sharp threshold. There is, however, a subtle difference in the timing of the response between type I models with saddle-node-onto-limit-cycle bifurcation and type II models with Hopf bifurcation. In models with Hopf bifurcation, the peak of the response is always reached with roughly the same delay, independently of the size of the input pulse. It is the amplitude of the response that increases rapidly but continuously; see Fig. 4.20b.

This is to be contrasted with the behavior of models with a saddle-node-onto-limit cycle behavior. As discussed above, the amplitude of the response of type I models is rather stereotyped: either there is an action potential or not. For input currents which are just above threshold, the action potential occurs, however, with an extremely long delay.

4.6 Separation of time scales and reduction to one dimension

Consider the generic two-dimensional neuron model given by Eqs. (4.4) and (4.5). We measure time in units of τ and take $R = 1$. Equations (4.4) and (4.5) are then

$$\frac{\mathrm{d}u}{\mathrm{d}t} = F(u,w) + I, \tag{4.33}$$

$$\frac{\mathrm{d}w}{\mathrm{d}t} = \varepsilon\, G(u,w), \tag{4.34}$$

where $\varepsilon = \tau/\tau_w$. If $\tau_w \gg \tau$, then $\varepsilon \ll 1$. In this situation the time scale that governs the evolution of u is much faster than that of w. This observation can be exploited for the analysis of the system. The general idea is that of a "separation of time scales;" in the mathematical literature the limit of $\varepsilon \to 0$ is called "singular perturbation." Oscillatory behavior for small ε is called a "relaxation oscillation."

What are the consequences of the large difference of time scales for the phase portrait of the system? Recall that the flow is in the direction of $(\dot{u}, \dot{w})$. In the limit of $\varepsilon \to 0$, all arrows in the flow field are therefore horizontal, except those in the neighborhood of the u-nullcline. On the u-nullcline, $\dot{u} = 0$ and arrows are vertical as usual. Their length, however, is only of order ε. Intuitively speaking, the horizontal arrows rapidly push the trajectory toward the u-nullcline. Only close to the u-nullcline are directions of movement other than horizontal possible. Therefore, trajectories slowly follow the u-nullcline, except at the knees of the nullcline where they jump to a different branch.

Excitability can now be discussed with the help of Fig. 4.21. A current pulse shifts the state of the system horizontally away from the stable fixed point. If the current pulse is small, the system returns immediately (i.e., on the fast time scale) to the stable fixed point. If the current pulse is large enough so as to put the system beyond the middle branch of

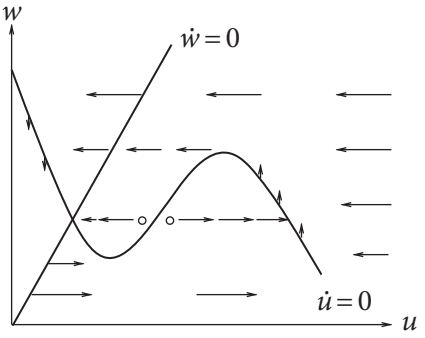

Fig. 4.21 Excitability in a type II model with separated time scales. The u-dynamics are much faster than the w-dynamics. The flux is therefore close to horizontal, except in the neighborhood of the u-nullcline (schematic figure). Initial conditions (circle) to the left of the middle branch of the u-nullcline return directly to the stable fixed point; a trajectory starting to the right of the middle branch develops a voltage pulse.

the u-nullcline, then the trajectory is pushed toward the right branch of the u nullcline. The trajectory follows the u-nullcline slowly upward until it jumps back (on the fast time scale) to the left branch of the u-nullcline. The "jump" between the branches of the nullcline corresponds to a rapid voltage change. In terms of neuronal modeling, the jump from the right to the left branch corresponds to the downstroke of the action potential. The middle branch of the u-nullcline (where $\dot{u} > 0$) acts as a threshold for spike initiation; see Fig. 4.22.

If we are not interested in the shape of an action potential, but only in the process of spike initiation, we can exploit the separation of time scales for a further reduction of the two-dimensional system of equations to a *single* variable. Without input, the neuron is at rest with variables $(u_{\text{rest}}, w_{\text{rest}})^T$. An input current $I(t)$ acts on the voltage dynamics, but has no direct influence on the variable w. Moreover, in the limit of $\varepsilon \ll 1$, the influence of the voltage u on the w-variable via Eq. (4.34) is negligible. Hence, we can set $w = w_{\text{rest}}$ and summarize the voltage dynamics of spike initiation by a singe equation

$$\frac{\mathrm{d}u}{\mathrm{d}t} = F(u, w_{\text{rest}}) + I\,. \tag{4.35}$$

Equation (4.35) is the basis of the nonlinear integrate-and-fire models that we will discuss in Chapter 5.

In a two-dimensional neuron model with separation of time scales, the upswing of the spike corresponds to a rapid horizontal movement of the trajectory in the phase plane. The upswing is therefore correctly reproduced by Eq. (4.35). The recovery variable departs from its resting value w_{rest} only during the return of the system to rest, after the voltage has (nearly) reached its maximum (Fig. 4.22a). In the one-dimensional system, the downswing of the action potential is replaced by a simple reset of the voltage variable, as we shall see in the next chapter.

https://doi.org/10.1017/CBO9781107447615.005 Published online by Cambridge University Press

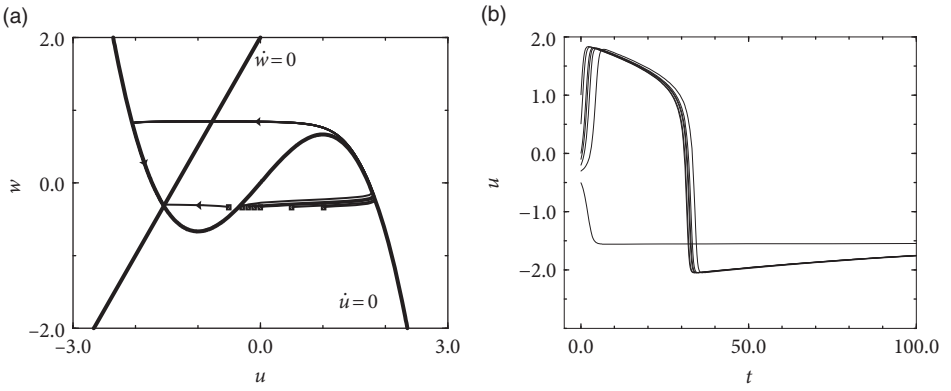

Fig. 4.22 FitzHugh–Nagumo model with separated time scales. All parameters are identical to those of Fig. 4.20 except for ε in Eq. (4.34) which has been reduced by a factor of 10. (a) A trajectory which starts to the left-hand side of the middle branch of the u-nullcline returns directly to the rest state; all other trajectories develop a pulse. (b) Owing to slow w-dynamics, pulses are much broader than in Fig. 4.20.

Example: Piecewise linear nullclines

Let us study the piecewise linear model shown in Fig. 4.23,

$$\frac{\mathrm{d}u}{\mathrm{d}t} = f(u) - w + I, \tag{4.36}$$

$$\frac{\mathrm{d}w}{\mathrm{d}t} = \varepsilon\,(bu - w), \tag{4.37}$$

with $f(u) = au$ for $u < 0.5$, $f(u) = a\,(1-u)$ for $0.5 < u < 1.5$ and $f(u) = c_0 + c_1 u$ for $u > 1.5$ where $a, c_1 < 0$ are parameters and $c_0 = -0.5a - 1.5c_1$. Furthermore, $b > 0$ and $0 < \varepsilon \ll 1$.

The rest state is at $u = w = 0$. Suppose that the system is stimulated by a short current pulse that shifts the state of the system horizontally. As long as $u < 1$, we have $f(u) < 0$. According to (4.36), $\dot{u} < 0$ and u returns to the rest state. For $u < 0.5$ the relaxation to rest is exponential with $u(t) = \exp(at)$ in the limit of $\varepsilon \to 0$. Thus, the return to rest after a small perturbation is governed by the *fast* time scale.

If the current pulse moves u to a value larger than unity, we have $\dot{u} = f(u) > 0$. Hence the voltage u increases and a pulse is emitted. That is to say, $u = 1$ acts as a threshold. Hence, under the assumption of a strict separation of time scales, this neuron model does have a threshold when stimulated with pulse input. The threshold sits on the horizontal axis $w = 0$ at the point where $\dot{u} = 0$.

Let us now suppose that the neuron receives a weak and constant background current during our threshold-search experiments. A constant current shifts the u-nullcline vertically upward. Hence the point where $\dot{u} = 0$ shifts leftward and therefore the voltage

https://doi.org/10.1017/CBO9781107447615.005 Published online by Cambridge University Press

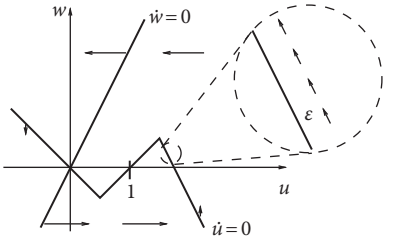

Fig. 4.23 Piecewise linear model with separation of time scale. The inset shows the trajectory (arrows) which follows the u-nullcline at a distance of order ε where $\varepsilon \ll 1$ is the ratio of the time scale of the u-dynamics and that of the w-dynamics in unit-free coordinates; see Eq. (4.37).

threshold for pulse stimulation sits now at a lower value. Again, we conclude that the threshold value we find depends on the stimulation protocol.

4.7 Summary

The four-dimensional model of Hodgkin–Huxley can be reduced to two dimensions under the assumption that the m-dynamics are fast compared with u, h, and n, and that the latter two evolve on the same time scale. Two-dimensional models can readily be visualized and studied in the phase plane.

As a first application of phase plane analysis, we asked whether neuron models have a firing threshold – and found that the answer is something like "No, but ... ." The answer is "No," because the threshold value depends on the stimulation paradigm. The voltage threshold derived with short current pulses is different from that found with constant current or slow ramps. In type II models the onset of repetitive firing at the rheobase current value starts with nonzero frequency. Type I models exhibit onset of repetitive firing with zero frequency. The transition to repetitive firing in type I models arises through a saddle-node-onto-limit-cycle bifurcation whereas several bifurcation types can give rise to a type II behavior.

The methods of phase plane analysis and dimension reduction are generic tools and will also play a role in several chapters of Parts II and IV of this book. In particular, the separation of time scales between the fast voltage variable and the slow recovery variable enables a further reduction of neuronal dynamics to a one-dimensional nonlinear integrate-and-fire model, a fact which we will exploit in the next chapter.

Literature

An in-depth introduction to dynamical systems, stability of fixed points, and (un)stable manifolds can be found, for example, in the book of Hale and Koçac (1991). The book by Strogatz (1994) presents the theory of dynamical systems in the context of various problems of physics, chemistry, biology, and engineering. A wealth of applications of dynamical systems to various (mostly non-neuronal) biological systems can be found in the comprehensive book by Murray (1993), which also contains a thorough discussion of

https://doi.org/10.1017/CBO9781107447615.005 Published online by Cambridge University Press

the FitzHugh–Nagumo model. Phase plane methods applied to neuronal dynamics are discussed in the clearly written review paper of Rinzel and Ermentrout (1998) and in the book by Izhikevich (2007b).

The classification of neuron models as type I and type II can be found in Rinzel and Ermentrout (1998) and in Ermentrout (1996), and systematically in Izhikevich (2007b). The steps of dimensionality reduction are presented in Kepler *et al*. (1992).

Exercises

1. **Inhibitory rebound.**
   (a) Draw on the phase plane a schematic representation of the nullclines and flow for the piecewise linear FitzHugh–Nagumo (Eqs. (4.36) and (4.37)) with parameters $a = c_1 = -1$ and $b = 2$, and mark the stable fixed point.
   (b) A hyperpolarizing current is introduced very slowly and increased up to a maximal value of $I = -2$. Calculate the new value of the stable fixed point. Draw the nullclines and flow for $I = -2$ on a different phase plane.
   (c) The hyperpolarizing current is suddenly removed. Use the phase planes in (a) and (b) to find out what will happen. Draw schematically the evolution of the neurons state as a membrane potential time-series and as a trajectory in the phase plane. Use $\varepsilon = 0.1$.
   Hint: The resting state from b is the initial value of the trajectory in c.
2. **Separation of time scales and quasi-stationary assumption.**
   (a) Consider the following differential equation:

$$\tau \frac{\mathrm{d}x}{\mathrm{d}t} = -x + c, \tag{4.38}$$

   where c is a constant. Find the fixed point of this equation. Determine the stability of the fixed point and the solution for any initial condition.
   (b) Suppose that c is now piecewise constant:

$$c = c(t) = \begin{cases} 0 & \text{for} t < 0 \\ c_0 & \text{for} 0 \le t \le 1 \\ 0 & \text{for} t > 1. \end{cases} \tag{4.39}$$

   Calculate the solution $x(t)$ for the initial condition $x(t = -10) = 0$.
   (c) Now consider the linear system:

$$\begin{aligned} \frac{\mathrm{d}u}{\mathrm{d}t} &= f(u) - m, \\ \varepsilon \frac{\mathrm{d}m}{\mathrm{d}t} &- m + c(u). \end{aligned} \tag{4.40}$$

   Exploit the fact that $\varepsilon << 1$ to reduce the system to one equation. Note the similarity with the equations in (a) and (b).
3. **Separation of time scale and relaxation oscillators.**
   (a) Show that in the piecewise linear neuron model defined in Eqs. (4.36) and (4.37) the trajectory evolves parallel to the right branch of the u-nullcline, shifted upward by a distance of order ε (Fig. 4.23) or parallel to the lifted branch of the u-nullcline, shifted downward by a distance of order ε.
   Hint: If the u-nullcline is given by the function $f(u)$, set $w(t) = f[u(t)] + \varepsilon x(t)$ where $x(t)$ is the momentary distance and study the evolution of $\mathrm{d}u/\mathrm{d}t$ and $\mathrm{d}w/\mathrm{d}t$ according to the differential equations of u and w. At the same time, under the assumption of parallel movement, $x(t)$ is

https://doi.org/10.1017/CBO9781107447615.005 Published online by Cambridge University Press

a constant and the geometry of the problem in the two-dimensional phase space tells us that $\mathrm{d}w/\mathrm{d}t = (\mathrm{d}f/\mathrm{d}u)\,(\mathrm{d}u/\mathrm{d}t)$. *Show that this leads to a consistent solution for the distance x.*
(b) What is the time course of the voltage $u(t)$ *while the trajectory follows the branch?*

https://doi.org/10.1017/CBO9781107447615.005 Published online by Cambridge University Press